

Modified rougan decoction alleviates lipopolysaccharide-enrofloxacin-induced hepatotoxicity via activating the Nrf2/ARE pathway in chicken

Wenjia Wang, Yu Shi, Tianxin Qiu, Jinwu Meng, Jinxue Ding, Weiran Wang, Desheng Wu, Kun Li, Jiaguo Liu,¹ and Yi Wu

Institute of Traditional Chinese Veterinary Medicine, College of Veterinary Medicine, Nanjing Agricultural University, Nanjing 210095, PR China

ABSTRACT Liver injury plays a heavy burden on the chicken industry. Although modified rougan decoction is a prescription for the treatment of liver disease based on the classical prescription of rougan decoction (containing peony and licorice). However, the effect and mechanism of modified rougan decoction on the liver remain unclear. In this study, the effects of the water extracts (MRGD) and the alcohol precipitates of water extracts (MRGDE) against lipopolysaccharide-enrofloxacin (LPS-ENR)-induced hepatotoxicity were discussed in vivo and in vitro. The isolated hepatocytes and 128 one-day-old Hyline chickens were considered research objects. The indices of liver injury and oxidative stress were evaluated by hematoxylin and eosin (H&E) stained and the assay kits, and the nuclear erythroid 2-related factor 2 (Nrf2)/antioxidant responsive element (ARE) pathway was detected by the RT-PCR, western blot, and immunofluorescence tests. All data were analyzed using the IBM SPSS 20.0 software. In vivo, the

structural integrity of the liver was maintained, AST, ALT, and MDA levels were decreased, and antioxidant enzymes were increased, confirming that the oxidative stress was reduced and liver injury was alleviated. Correspondingly, MRGD and MRGDE were observed to improve cell viability and decrease lactate dehydrogenase (LDH) in vitro, and the cell oxidative damage was reduced. In addition, the nuclear translocation of Nrf2 was improved significantly, and the mRNA and protein expression levels of the related genes were upregulated. In conclusion, MRGD and MRGDE can exert a protective effect against LPS-ENR-induced hepatotoxicity by activating the Nrf2/ARE pathway, which might be a potential therapeutic prescription for preventing or treating liver injury. Notably, no significant difference was found between the 2 extracts, suggesting that a depth extraction method did not always improve the efficacy of natural medicine. Our results provided new insights into finding effective hepatoprotective medicine.

Key words: chicken, Chinese herbs, antioxidant, Nrf2, liver injury

2023 Poultry Science 102:102404

<https://doi.org/10.1016/j.psj.2022.102404>

INTRODUCTION

The liver is the largest visceral organ in the body and plays a vital role in dyspepsia, biosynthesis, metabolism, and detoxification (Ren et al., 2019). However, liver health is susceptible to various factors. For example, improper or excessive use of drugs, pathogen invasion, toxins, and so on (Begrache et al., 2011). Liver disease seriously affects animals' health. Enrofloxacin (ENR) is a fluoroquinolone and has been widely used to prevent or treat avian-associated bacterial infections. Long-term or excessive use of ENR increases the burden on the liver

and results in hepatotoxicity causing chemically driven liver damage. After infection with gram-negative bacteria, ENR treatment leads to the lysis of bacterial cell lipopolysaccharide (LPS) in the body, and its endotoxins aggravate liver damage (Gandhi, 2020). Previous studies have explored the related mechanisms of drugs and LPS leading to liver injury (Al-Dossari et al., 2020; Guo et al., 2020). Only a few drugs can be used for the treatment, and there are no obvious therapeutic effects. Therefore, new drugs and therapeutic strategies are needed to enhance therapeutic efficacy.

One of the causes of liver injury is cellular oxidative stress (Vera-Ramirez et al., 2011, 2013; Kucera et al., 2014), which subsequently induces inflammation, apoptosis, and liver fibrosis. Nuclear factor erythroid-2-related factor 2 (Nrf2) is the primary regulator of cell protection genes, maintaining intracellular homeostasis (Jadeja et al., 2016). Nrf2 is translocated into the

© 2022 The Authors. Published by Elsevier Inc. on behalf of Poultry Science Association Inc. This is an open access article under the CC BY-NC-ND license (<http://creativecommons.org/licenses/by-nc-nd/4.0/>).

Received September 17, 2022.

Accepted December 5, 2022.

¹Corresponding author: liujiaguo@njau.edu.cn

nucleus which regulates the antioxidant responsive element (**ARE**) gene expression to protect the cells from oxidative stress (He et al., 2008). Activation of Nrf2 effectively blocks or postpones oxidative stress-induced liver diseases.

Some drugs alleviate liver injury via the inhibition of oxidative stress. Rougan decoction (**RGD**) was recorded in the Treatise on Febrile Diseases (Shang Han Lun), which is a famous Chinese prescription containing *Paeoniae Radix* and *Glycyrrhizae Radix* (Bi et al., 2014). RGD has the effect of harmonizing the liver and spleen and relieving abdominal pain. Previous studies have demonstrated that RGD effectively treats liver diseases (Sun et al., 2020). **MRGD**, a new traditional Chinese medicine (**TCM**) prescription based on RGD, is composed of 7 herbs based on a certain proportion. **MRGDE** is a crude polysaccharide component obtained by the water extraction and alcohol precipitation method. Chinese herbal medicine contains abundant active ingredients, including flavonoids, polysaccharides, polyphenols, terpenoids, sterols, vitamins, and so on (Jiang et al., 2006; Lin, 2014; Liu et al., 2014; Ma et al., 2020). These bioactive components are known to have hepatoprotective, anti-inflammatory, and high antioxidant capacities (Lin, 2014; Torres et al., 2016; Bakr et al., 2017; He et al., 2019). Based on this research, we speculated that MRGD and MRGDE have an antioxidant effect and might alleviate liver disease (Peng et al., 2020).

Many herbs were well established to prevent and treat liver diseases; however, the scientific basis for MRGD and MRGDE hepatoprotective effects remains to be explored. In this study, LPS combined with ENR-induced hepatotoxicity model was used to evaluate the antioxidant stresses of MRGD and MRGDE in in vitro and in vivo, respectively. It is expected to provide potentially valuable TCM prescriptions for developing hepatoprotective drugs.

MATERIALS AND METHODS

Preparation of MRGD and MRGDE

The herbs were purchased from Nanjing Tongrentang Medicine Company (Nanjing, China) in this study.

MRGD was composed of 7 Chinese herbs (*Hypericum japonicum*, *Alisma orientalis*, *Paeonia lactiflora*, *Poria*, *Glycyrrhizae radix*, *Schisandra chinensis* fruit, and *Magnolia officinalis*). The herbs of MRGD (200 g) and 2 L of water were added to a beaker. After soaking for 45 min, the herbs were boiled and stewed for 2 h. After the liquid was filtered, the herb residue was added to 2 L of water for cooking the second time. The 2 liquids were mixed and concentrated to 200 mL.

Preparation of MRGDE: to reach a final 70% alcohol concentration (v/v), anhydrous ethanol was added to the prepared MRGD concentrate. After precipitation at 4°C for 12 h, the precipitate was obtained, dissolved in

deionized water, and deproteinized by the Seavage method (n-butanol:chloroform = 1:4). The solution of polysaccharide and Seavage reagent were mixed to a 5:1 ratio, and vibrated for 30 min at low-speed centrifugation, and repeated 3 times to remove the denatured protein (Yi et al., 2015; Tang et al., 2019). Finally, the total sugars of the MRGDE were determined to be $34.45 \pm 1.78\%$ by the phenol-sulfuric acid method, using glucose as the standard (Cuesta et al., 2003; Albalasmeh et al., 2013).

The lyophilized powders of MRGD (30 g, the rate of power/raw herbs was 15%) and MRGDE (8.8 g, the rate of power/raw herbs was 4.4%) were obtained by a vacuum freeze-drying machine (ShanghaiBiLang, Shanghai, China). The MRGD and MRGDE dry powders were dissolved in pure water. LPS (L2630, Sigma-Aldrich, St. Louis, MO) was dissolved in normal saline. ENR (SE8390, Solarbio, Beijing, China) was stored in a slightly alkaline aqueous solution.

Cell Culture and Treatment

Liver tissue was isolated from 14-day-old fertilized eggs and then digested with 0.20% trypsin (T2600000, Amresco, Spokane, WA). After washing thrice with D-Hank's solution, the cells were cultured in 10% FBS DMEM, inoculated in 96- or 6-well plates at $1 - 1.5 \times 10^5$ cells/mL for 24 h at 37°C with 5% CO₂.

The cells were cultured in MRGD, MRGDE, LPS, and ENR solutions (1% FBS DMEM) for 12 h at 37°C, respectively. Subsequently, the cell viability was detected by the MTT assay and measured to quantify by the $OD_{570\text{ nm}}$ (Rabkin, 2002; Li et al., 2014). The IC₅₀ values were calculated using the Prism software (GraphPad Prism 8 software, Inc., San Diego, CA) (Hurtado et al., 2019; Krakowian et al., 2021).

Detection of Cell Injury and Oxidative Stress Indices

To determine the effects of MRGD and MRGDE on cell injury and oxidative stress induced by LPS-ENR, the cells were inoculated in 6-well plates at 3×10^5 cells/mL and divided into 4 groups (BLANK, LPS-ENR, MRGD, and MRGDE groups). The drugs (MRGD, MRGDE) were added to the MRGD and MRGDE groups for 12 h, respectively. Then LPS (30 µg/mL) and ENR (125 µg/mL) were mixed and added to the LPS-ENR, MRGD, and MRGDE groups for 12 h, respectively. The cell viability was detected by the MTT assay and a lactate dehydrogenase (**LDH**) kit (BC0685, Solarbio, Beijing, China). The oxidative stress of cells was estimated by detecting the malondialdehyde (**MDA**) level (A003-4-1, Nanjing Jiancheng, Nanjing, China) and superoxide dismutase (**SOD**) (A001-3-2, Nanjing Jiancheng, Nanjing, China) and catalase (**CAT**) activities (A007-1-1, Nanjing Jiancheng, Nanjing, China) following the detection kits protocol of Nanjing Jiancheng Bioengineering Institute (Nanjing, China).

Detection of Intracellular ROS Level to Determine the Oxidative Stress in Hepatocyte

The detection of ROS level is one of the indicators of oxidative stress in cells. The content of ROS was evaluated by the DCFH-DA probe method (S0033S, Beyotime, Shanghai, China). After the cells were treated according to the above method, they were coincubated with a DCFH-DA probe (5 μ M/L) at 37°C for 30 min. The fluorescence signal of DCF (an oxidation product of DCFH-DA) by the Invitrogen EVOS FL Auto Imaging System (Thermo Fisher, Waltham, MA) was immediately observed. The ImageJ software was used to analyze the average fluorescence intensity of randomly selected regions.

Nuclear Localization of Nrf2 After Oxidative Stress by Immunofluorescence Staining

The cells were planted in 6-well plates at 1×10^5 cells/mL. After the influence of LPS-ENR, the cells were washed twice with PBS and fixed with 4% paraformaldehyde for 15 min. Then the cells were penetrated with 0.5% Triton X-100 for 20 min, re-washed in PBS, and blocked in PBS containing 5% BSA for 30 min. The primary or secondary antibody solutions were used, respectively. DAPI was used to stain nuclei for 5 min. Images were taken by using the Invitrogen EVOS FL Auto Imaging System.

Animals Grouping and Treatment

This study was conducted following the “Guidelines for Laboratory Animals” issued by the Ministry of Science and Technology (2006, Beijing, China) and was approved by the Animal Protection and Utilization Committee of Nanjing Agricultural University (#NJAU-Poult-2021101218). Male 1-day-old healthy Hyline hens were purchased from Jiangsu Province. The chickens were fed in the Experimental Animal Centre of Nanjing Agriculture University, with a 12 h light or dark cycle, constant temperature of $30 \pm 2^\circ\text{C}$, and adaptive feeding for 3 d before the research.

The chickens were randomly divided into 4 groups ($n = 32$): BLANK, LPS-ENR, MRGD, and MRGDE groups. The LPS-ENR, MRGD, and MRGDE groups were given aqueous ENR (20 mg/kg) for 3 d per chicken, and intraperitoneal injection of LPS (0.25 mg/kg) on the third day. At 1 h and 6 h after LPS injection, the protection groups were orally administered MRGD or MRGDE at a dose of 0.15 g/kg per chicken (raw herbs). The BLANK group was injected or orally given the same amount of normal saline or water.

After 24 h of LPS injection, the chickens were anaesthetized and killed ($n = 6$). The blood was collected to prepare serum, and the liver was immediately collected and washed with cold PBS, and stored at -80°C . Some liver sections were fixed in 4% neutral buffer formalin.

Biochemical Analysis of Serum and Histology Analysis to Detect Liver Injury in Chicken

To detect liver injury in chicken, the serum aspartate aminotransferase (AST), alanine aminotransferase (ALT), LDH, total protein (TP), and albumin (ALB) contents were determined by an automatic biochemical analyzer (UniCel Dx C 600 Synchron, Beckman Coulter, Brea, CA). The liver tissue was evaluated by optical microscope after being stained with hematoxylin and eosin (H&E).

Determination of Oxidative Damage Evaluation Index in Chicken Liver

Liver tissue was added to the cold PBS at 1:10 (w/v), homogenized, and centrifuged at $3,000 \times g$, for 10 min. Then the supernatant was collected to measure the activities of antioxidant enzymes SOD and CAT and the level of MDA following the detection kits protocol of Nanjing Jiancheng Bioengineering Institute (Nanjing, China).

Real-Time Quantitative PCR and Western Blot Analyses to Detect the Nrf2/IARE Pathway

Total RNA of the cells and liver tissues were extracted by the Trizol method. The concentration was determined by the NanoDrop 2000 Spectrometer (Thermo Scientific, Waltham, MA). Total RNA was transcribed into cDNA using a reverse transcription kit produced by Vazyme of China. The mRNA expressions of the antioxidant genes were detected by quantitative real-time qPCR (QuantStudio7 Flex, Thermo Fisher, Waltham, MA), and GAPDH was used as the internal control. The $2^{-\Delta\Delta\text{CT}}$ method was used to analyze the relative gene expression data. All primers were synthesized from Shanghai Generey Biotech Co. Ltd. (Shanghai, China) (Table 1).

The cells and liver tissues were collected with RIPA Lysis Buffer (P0013B, Beyotime, Beijing, China) containing PMSF protease inhibitor. The protein concentration of samples was determined by the BCA protein

Table 1. Primers used in qRT-PCR.

Gene	Primer sequence (5' to 3')
Nrf2-F	GATGTCACCCTGCCCTTAG
Nrf2-R	CTGCCACCATGTTATTCC
NQO1-F	TCCCGGAGCAGAAGAAGATTGAAG
NQO1-R	GGTGGTAGTGACAGCATGGC
HO-1-F	ACGTCGTTGGCAAGAAGCATCC
HO-1-R	TTGAACTGGTGGCGTTGGAGAC
CAT-F	GTTGGCGGTAGGAGTCTGGTCT
CAT-R	GTGGTCAAGGCATCTGGCTTCTG
SOD-F	TTGTCTGATGGAGATCATGGCTTC
SOD-R	TGCTTGCCTTCAGGATTAAGTGA
GPX1-F	CAAAGTTGCGGTCAGTGGGA
GPX1-R	AGAGTCCCAGGCCTTTACTACTTTC
GAPDH-F	CAACACAGTGTCTGTGGTGGTA
GAPDH-R	ATCGTACTCCTGCTTGTGATCC

detection kit (P0010, Beyotime, Beijing, China). The standard western blot analysis was performed with primary antibodies for the detection of Nrf2 (1:500, AF0639, Affinity), NQO1 (1:500, A0047, ABclonal), GPX1 (1:500, A1110, ABclonal), and β -actin (1:2,000, AC038, ABclonal). An ultrasensitive chemiluminescence gel imaging system (Bio-Rad, Hercules, CA) was used to detect the bands, and the ImageJ software was used to analyze the gray value quantitatively.

Statistical Analysis

All data came from at least 3 independent repeated trials and were analyzed using the IBM SPSS 20.0 software (Ammonk IBM, New York, NY). One-way analysis

of variance was used for comparison between groups, and Duncan's multiple range test was used for different analyses. All values were expressed as mean \pm SD. $P < 0.05$ and the 95% confidence interval indicated that the difference was statistically significant.

RESULTS

The Cell Viability and LDH Activity Were Changed by the Treatment of MRGD and MRGDE in Injured Hepatocytes

The MTT assay showed that the cell viability was decreased in a dose-dependent manner after LPS (10, 20, 40, 60, 80, 100, 120 $\mu\text{g}/\text{mL}$) or ENR (15.63, 31.25,

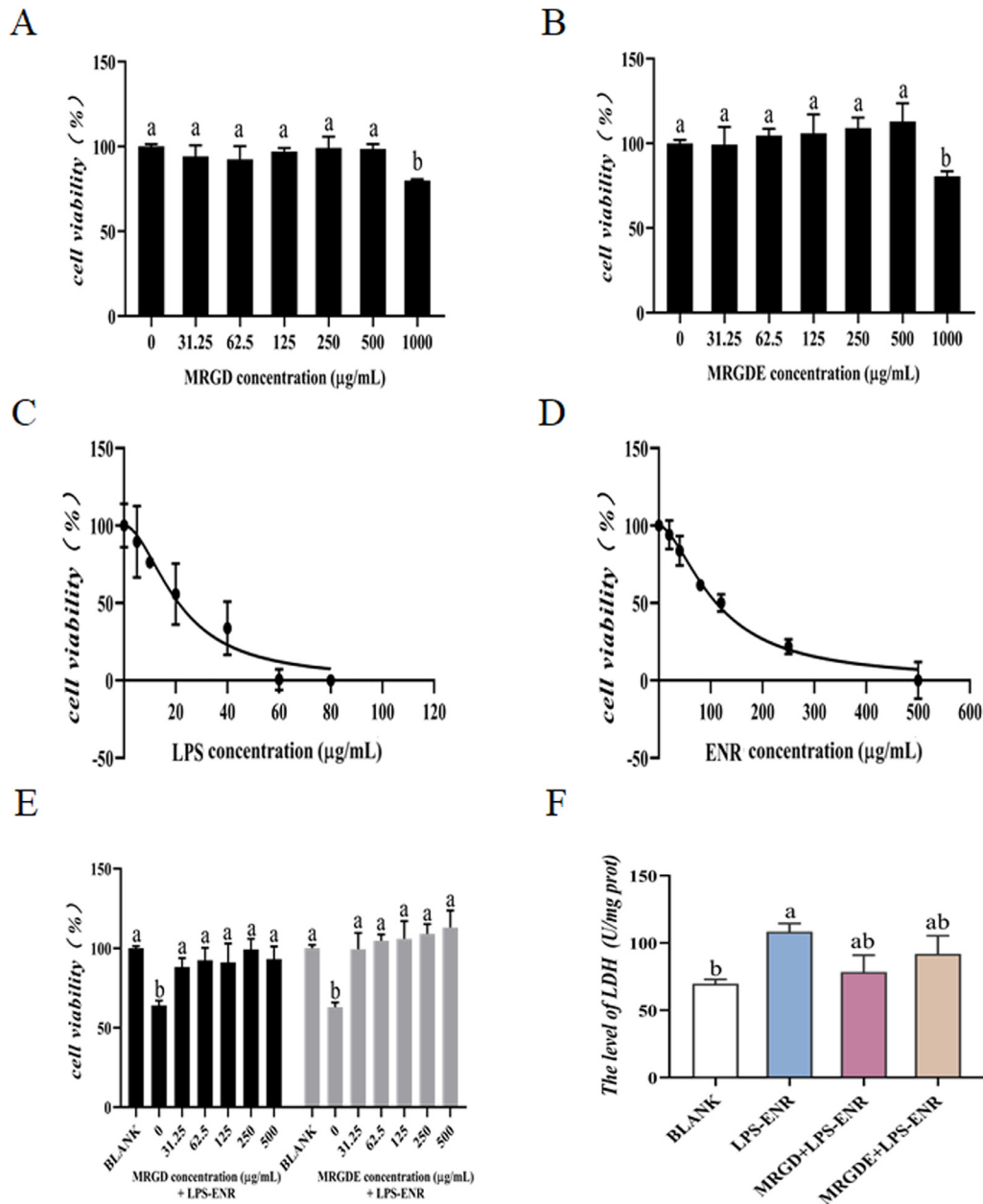


Figure 1. The cell viability was detected by MTT assay, and the LDH activity was assessed in injured hepatocytes. (A) MRGD affected cell viability. (B) MRGDE affected cell viability. (C) LPS affected cell viability. (D) ENR affected cell viability. (E) Effect of MRGD and MRGDE against the LPS-ENR in vitro. (F) The level of LDH activity in cells. Values are mean \pm SD. ^{a, b}Bars without the same superscripts differ significantly ($P < 0.05$).

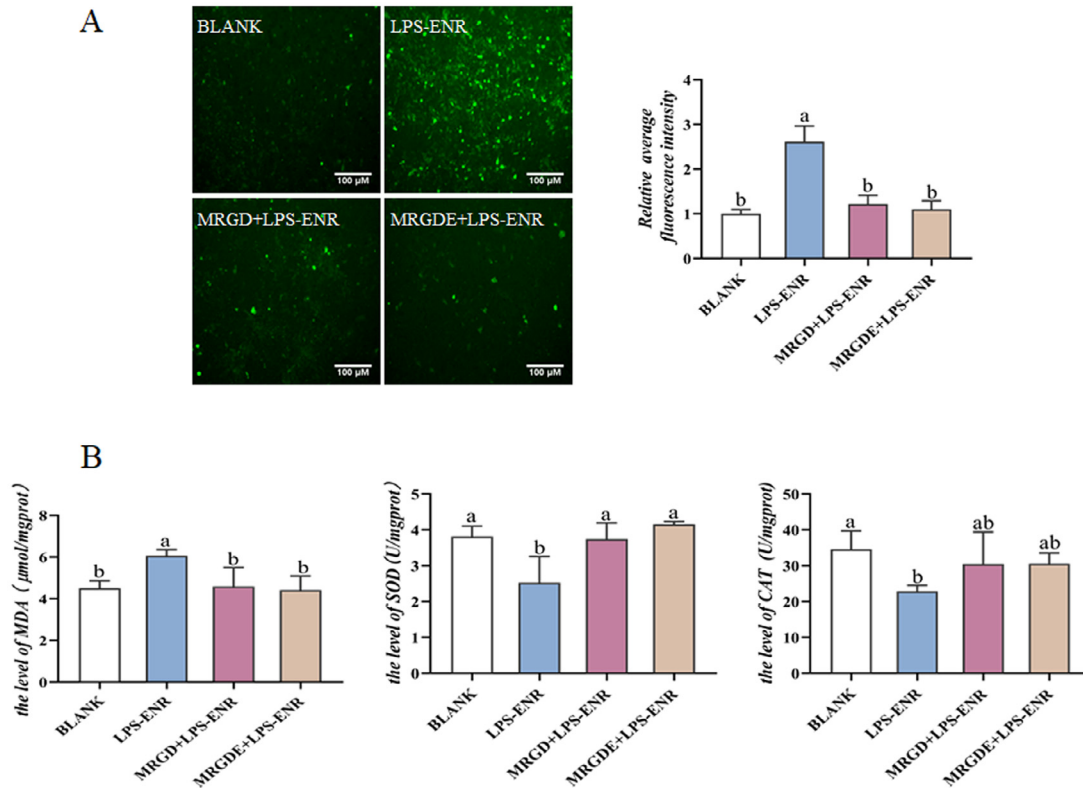


Figure 2. Oxidative stress occurred in cells. (A) The result of ROS immunofluorescence, with 3 images in each group. (B) Detection of MDA, CAT, and SOD levels in cells by the kit. Data are mean \pm SD. ^{a,b}Bars without the same superscripts differ significantly ($P < 0.05$).

62.5, 125, 250, 500 $\mu\text{g}/\text{mL}$) treatment, the results of IC₅₀ showed LPS (21.12 $\mu\text{g}/\text{mL}$) and ENR (111 $\mu\text{g}/\text{mL}$), respectively (Figure 1C and D). When the concentration of LPS-ENR was 30/125 $\mu\text{g}/\text{mL}$, the number of living cells was significantly decreased, and the cell viability was $63.00 \pm 2.97\%$ (Figure 1E). After MRGD and MRGDE (250 $\mu\text{g}/\text{mL}$) treatments, the cell viability was $91.13 \pm 11.86\%$ and $105.90 \pm 11.11\%$, which were similar to BLANK group ($P > 0.05$), respectively. The results showed that there were significant differences with the LPS-ENR group ($P < 0.05$), indicating that MRGD and MRGDE can protect (Figure 1A, B, and E). With the individual inoculation of LPS-ENR at 30/125 $\mu\text{g}/\text{mL}$, LDH activity was significantly lower than that of the BLANK group, while the LDH levels were decreased by MRGD and MRGDE (Figure 1F). These results showed that MRGD and MRGDE reduced hepatocyte injury.

MRGD and MRGDE Had an Antioxidant Effect in LPS-ENR-Induced Chicken Hepatocytes Injury

For further confirmation of ameliorating the oxidative stress, we measured the level of ROS in cultured hepatocytes with the fluorescence probe method. According to the fluorescence intensity, the level of ROS in the LPS-ENR group was significantly higher than that of the BLANK group ($P < 0.05$), indicating the increase in the accumulation of ROS levels after LPS-ENR stimulation.

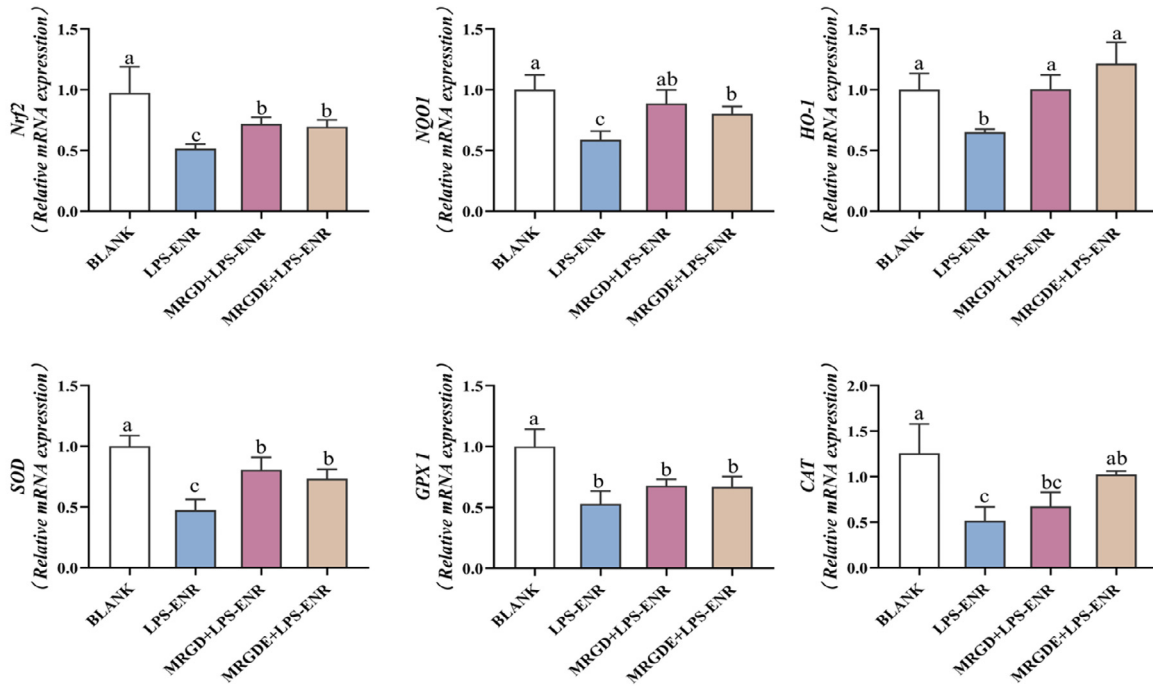
Compared with the LPS-ENR group, the fluorescence intensities of the MRGD and MRGDE groups were weaker ($P < 0.05$). There was no significant difference between the BLANK and the 2 drug groups ($P > 0.05$) (Figure 2A).

The excessive production of ROS indicated that oxidative stress occurs in the cells. We further detected the levels of MDA and antioxidant enzymes in cells. The results showed that the MDA content in the LPS-ENR group was significantly higher ($P < 0.05$), and the activities of SOD and CAT in the cells were lower than that of the BLANK group ($P < 0.05$). After MRGD or MRGDE pretreatments, the MDA, SOD, and CAT levels recovered to the normal level (Figure 2B).

The Treatments of MRGD and MRGDE Alleviated the Oxidative Stress Via Upregulating Nrf2/IARE Signals Pathway In Vitro

In in vitro experiment, the mRNA expression levels of antioxidant genes were obviously decreased in the LPS-ENR group ($P < 0.05$), and the results showed that oxidative stress might occur (Figure 3A). Notably, the expression levels of antioxidant proteins in the LPS-ENR group were significantly lower than that of the BLANK group ($P < 0.05$), which confirmed the occurrence of oxidative stress at the protein level (Figure 3B). MRGD and MRGDE improved the Nrf2 and GPX1

A



B

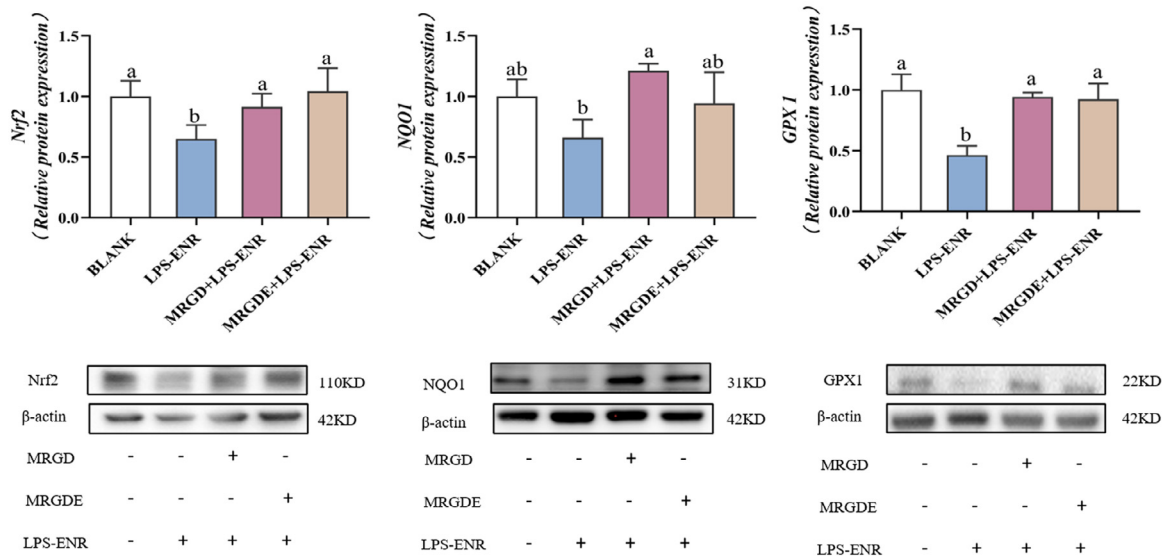


Figure 3. The treatment of MRGD and MRGDE alleviated oxidative stress by upregulating the Nrf2/ARE signal pathway in cells. (A) The mRNA expression levels of Nrf2/ARE signal pathway genes (Nrf2, NQO-1, HO-1, SOD, GPX1, CAT) in cells. (B) The protein expression levels of Nrf2, NQO1, and GPX1 in cells. Data are mean \pm SD. ^{a-c}Bars without the same superscripts differ significantly ($P < 0.05$).

proteins levels ($P < 0.05$), and the MRGDE upregulated the level of NQO1 protein ($P > 0.05$). In brief, the results showed that oxidative stress was reduced via activating the mRNA and protein expression levels of Nrf2/ARE pathway genes by MRGD or MRGDE pretreatment.

MRGD and MRGDE Activated Nuclear Translocation of Nrf2 in Cells

We examined whether MRGD and MRGDE protect the cell from injury by activating Nrf2, and the effects of

Nrf2 translocation from cytoplasm to nucleus were evaluated (Figure 4). It was observed that the Nrf2 transfer was blocked by the treatment with LPS-ENR alone, while MRGD and MRGDE pretreatments changed the level of Nrf2 in the cytoplasm and nucleus. The results showed that Nrf2 was mainly located in the cytoplasm of LPS-ENR group cells using an immunofluorescence assay. These data demonstrated that MRGD and MRGDE pretreatments alleviated the LPS-ENR-mediated obstruction in the translocation of Nrf2 protein in hepatocytes and increased its localization in the nucleus (Figure 4).

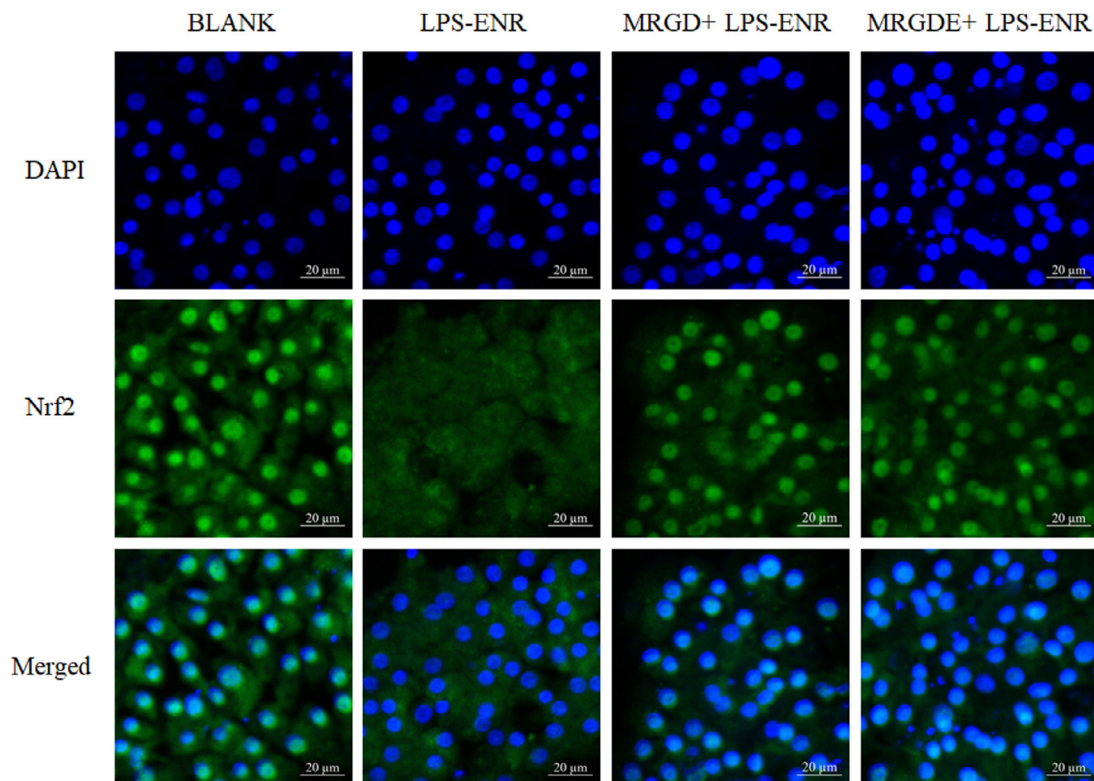


Figure 4. MRGD and MRGDE activated nuclear translocation of Nrf2 protein in cells by immunofluorescence assay. MRGD and MRGDE activate the nuclear translocation of Nrf2 in cells. DAPI (blue) was used to label the nucleus; green was used to label the protein of Nrf2 in cells. Observation of Nrf2 fluorescence by fluorescence microscope, with 3 images in each group. Scale bar: 20 μm .

MRGD and MRGDE Ameliorated LPS-ENR-Induced Liver Injury by Inhibiting the Oxidative Stress In Vivo

The serum biochemical indices and structure of liver tissue were evaluated. Compared with the BLANK group, the AST and ALT levels in the LPS-ENR group were remarkably increased ($P < 0.05$), while the LPS-ENR did not change the levels of TP and ALB in this study. After drug treatment, the impacts on AST and ALT were significantly decreased by MRGD ($P < 0.05$), and lightly alleviated by MRGDE ($P > 0.05$) (Table 2).

Compared with the BLANK group, the liver in the LPS-ENR group was slightly expanded and showed hemorrhage; however, the liver had improved in the treatment groups. The H&E-staining showed that the intercellular boundary of the hepatic lobular structure in the chicken liver tissue was clear, and there was no inflammation, congestion, bleeding, or exudation in the BLANK group (Figure 5A). The LPS-ENR group showed deeply stained nuclei, inflammatory cell infiltration, vascular swelling, hemorrhage, and necrosis (Figure 5A); however, the MRGD and MRGDE groups showed slight pathological changes (Figure 5A). The ratio of the liver/body of the LPS-ENR group was significantly increased compared with the BLANK group ($P < 0.05$), and indicated that the liver was swollen, which was consistent with the H&E results (Figure 5B). Interestingly, MRGD and MRGDE maintained the normal liver structure. These results showed that MRGD and

MRGDE had a certain inhibition action on the LPS-ENR-induced chicken liver injury.

Specifically, the MDA level in the LPS-ENR group was significantly higher than that of the BLANK group ($P < 0.05$) (Figure 5C), and the activities of SOD and CAT were significantly lower ($P < 0.05$) (Figure 5D ~ E). Compared with the LPS-ENR group, MDA levels were decreased in MRGD and MRGDE groups ($P < 0.05$); however, it did not decrease to the normal level of the BLANK group ($P < 0.05$) (Figure 5C). The SOD levels were improved markedly with the treatments of MRGD and MRGDE ($P < 0.05$); there was a marked increase in the CAT activity, but it remained nonsignificant (Figure 5E). These results showed that MRGD and MRGDE promote the activity of antioxidant enzymes.

MRGD and MRGDE Activated the Nrf2/ARE Pathway to Attenuate the LPS-ENR-Induced Liver Oxidative Stress In Vivo

Among the Nrf2/ARE signal-related genes detected in chicken liver, the mRNA expression levels of 4 genes were affected by the LPS-ENR treatment (Figure 6A), the mRNA expression levels of NQO1, HO-1, SOD, and GPX1 genes were downregulated by LPS-ENR alone ($P < 0.05$). MRGD effectively increased the mRNA expression levels of SOD and GPX1 genes, while the MRGDE improved the mRNA expression levels of NQO1 and HO-1 genes after LPS-ENR treatment ($P <$

Table 2. Biochemical indexes in serum.

Index	BLANK	LPS-ENR	MRGD+LPS-ENR	MRGDE+LPS-ENR
AST (U/L)	233.53 ± 11.00 ^b	297.93 ± 15.38 ^a	241.10 ± 8.88 ^b	266.97 ± 21.50 ^{ab}
ALT (U/L)	7.17 ± 0.85 ^c	11.00 ± 0.25 ^a	8.33 ± 0.67 ^{bc}	9.83 ± 0.41 ^{ab}
TP (g/L)	34.43 ± 1.30 ^a	26.63 ± 0.95 ^b	29.23 ± 0.74 ^b	29.63 ± 1.32 ^b
ALB (g/L)	12.50 ± 0.68 ^a	10.73 ± 0.77 ^a	11.33 ± 0.54 ^a	10.87 ± 0.61 ^a

Abbreviations: ALB, albumin; ALT, alanine aminotransferase; AST, aspartate aminotransferase; TP, total protein. Values are mean ± SD.

^{a-c}Bars in the same row without the same superscripts differ significantly ($P < 0.05$).

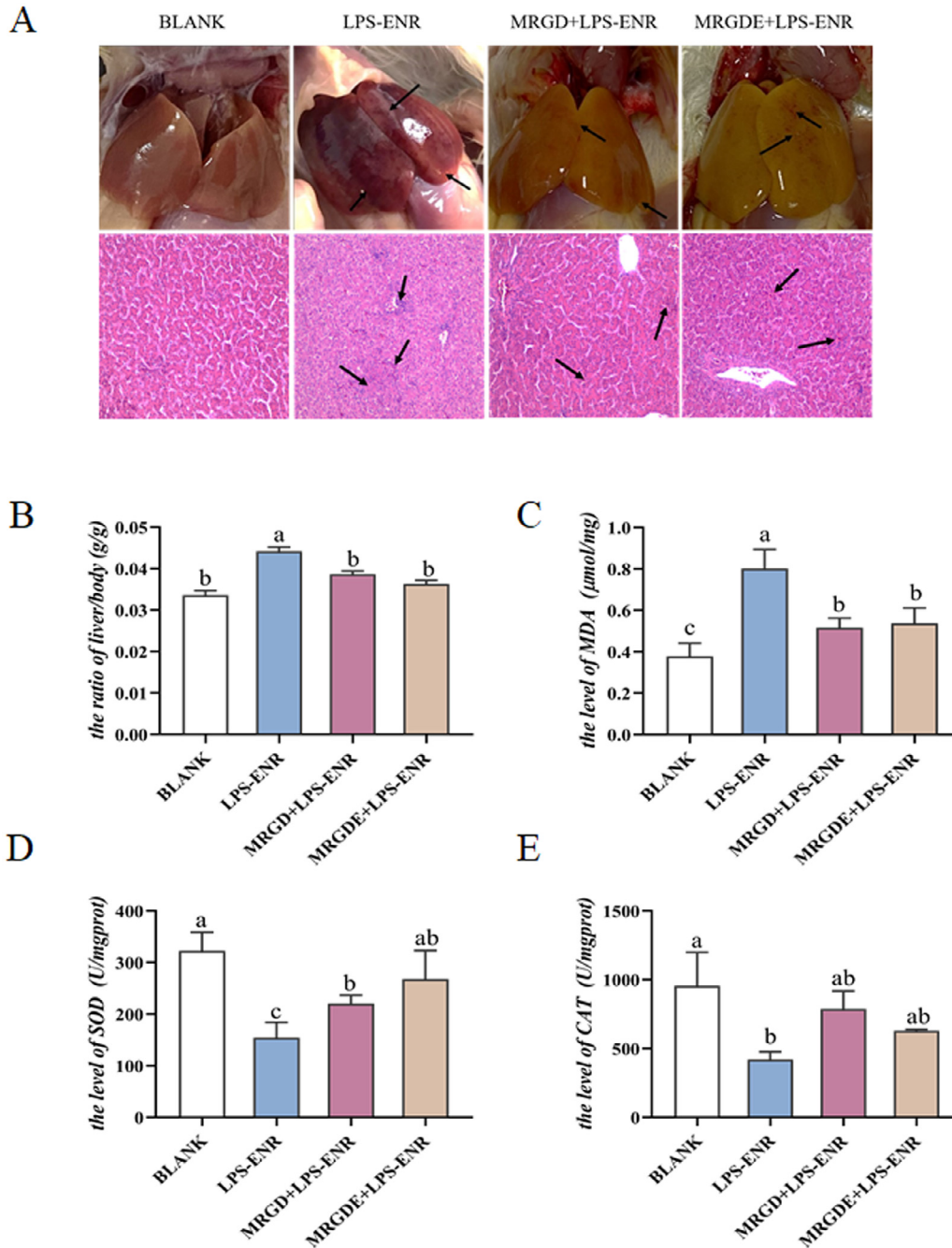
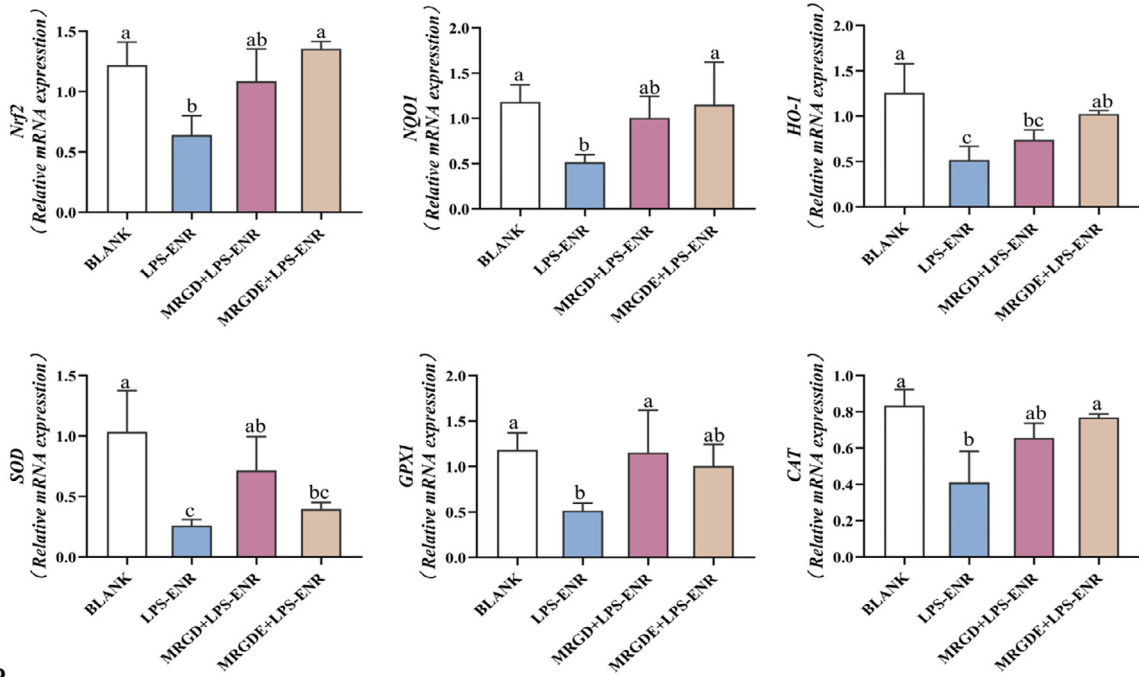


Figure 5. MRGD and MRGDE ameliorated LPS-ENR-induced liver injury by inhibiting oxidative stress in chicken. (A) Effects of MRGD and MRGDE on histopathology of chicken liver. Liver sections were stained with hematoxylin and eosin. Black arrow: hemorrhage, necrosis, and inflammatory infiltration in liver tissue; Scale bar: 100 μ m. (B) Hepatic index of each group. Organ ratio = organ weight/body weight. (C) MRGD and MRGDE affected the MDA levels in chicken liver. (D, E) Effects of the antioxidant enzyme SOD and CAT levels. Values are mean \pm SD. ^{a-c}Bars without the same superscripts differ significantly ($P < 0.05$).

A



B

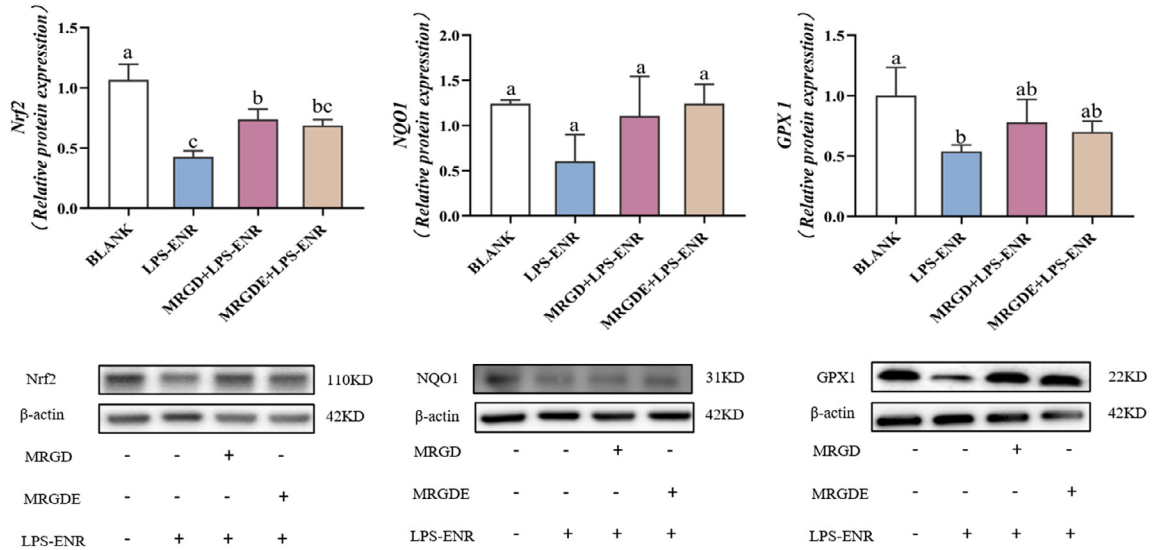


Figure 6. MRGD and MRGDE activated the Nrf2/ARE pathway to attenuate the LPS-ENR-induced liver oxidative stress in chickens. (A) The mRNA expression levels of the Nrf2/ARE signaling pathway gene. (B) Effect of MRGD and MRGDE on the protein expression levels of the Nrf2/ARE signaling pathway (Nrf2, NQO1, and GPX1) in chicken liver. Data are mean \pm SD. ^{a-c}Bars without the same superscripts differ significantly ($P < 0.05$).

0.05). In addition, the western blot results showed that compared with the BLANK group, the expression levels of Nrf2 and GPX1 proteins were significantly decreased in the LPS-ENR group ($P < 0.05$) (Figure 6B). It is worth noting that compared with the LPS-ENR group, the expression levels of related proteins were improved in the MRGD and MRGDE groups (Figure 6A and B).

DISCUSSION

For thousands of years, herbal and traditional medicines have been used to prevent and treat diseases

worldwide, and they are the sources of many prescriptions and new drugs (Wu et al., 2017). In recent years, a variety of TCM prescriptions for the treatment of liver diseases have been widely studied, such as Huangqi and Xiaochaihu decoctions (Zhang et al., 2017; Zhao et al., 2017; Xi et al., 2018). In addition, there are many TCM extracts, such as ethanol precipitate (polysaccharide) hepatoprotective, that have received some researchers' attention (Wu et al., 2011, 2020; Yuan et al., 2018). In this study, the hepatoprotective effects of the water extract (MRGD) and ethanol precipitation extract (MRGDE) were compared. Two kinds of drugs showed excellent hepatoprotective effects in vivo and in vitro,

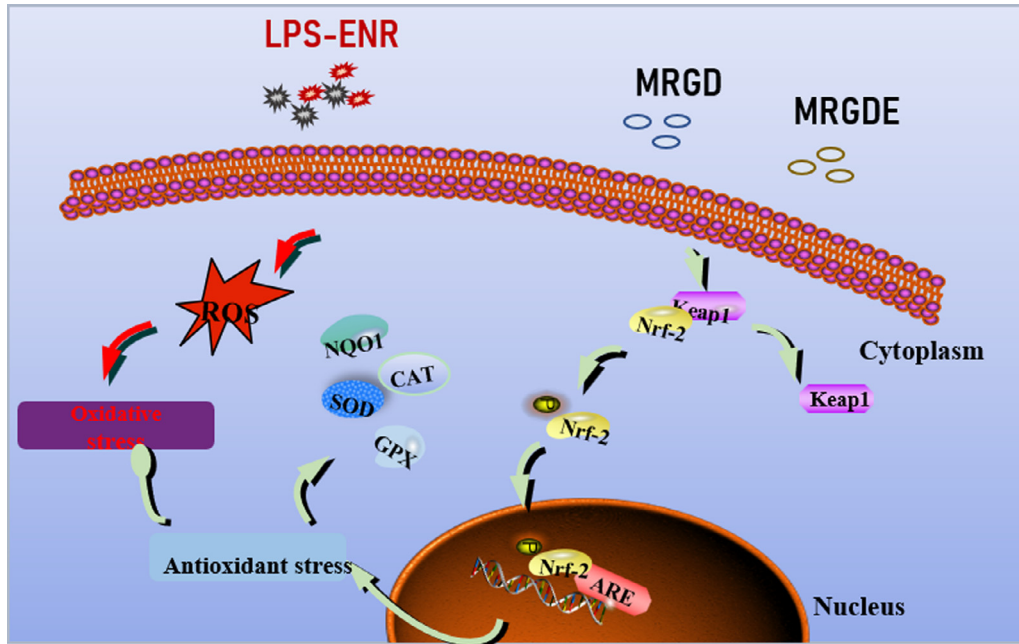


Figure 7. The relevant mechanism diagram of this study. This figure shows that the Nrf2/ARE signaling pathway was possibly activated by the MRGD and MRGDE.

reduced the levels of ALT and AST in serum (Table 2), decreased the levels of LDH activity (Figure 1F), and the liver tissue structure tended to be normal (Figure 5A). The results showed that the 2 drugs suppressed the liver injury caused by LPS-ENR to a certain extent, and the MRGD group also achieved as good effects as the MRGDE group, indicating that the polysaccharide components in the water extract played a vital role, and the over-extraction of herbs did not necessarily improve the effectiveness of drugs.

Oxidative stress can induce severe liver injury. MDA is one of the major products of lipid peroxidation induced by ROS, which is directly related to liver damage. It is reported that the MDA level in chicken was increased while exposed to LPS (Lee et al., 2017; Figure 5C). In this study, the occurrence of oxidative stress has been confirmed in the LPS-ENR-induced liver injury and cell model. In *in vitro* experiments, the level of ROS was increased in the LPS-ENR group (Figure 2A), and the LDH and MDA (Figures 1F and 2B) levels were significantly increased. Notably, MRGD and MRGDE decreased the levels of LDH and MDA and improved the activities of SOD and CAT (Figure 2B), suggesting that MRGD or MRGDE had a restraining effect on the LPS-ENR-induced cell injury. The antioxidant activities of MRGD and MRGDE at the cellular level have been verified. *In vivo*, LPS-ENR caused hepatocyte degeneration and necrosis by inducing oxidative stress, while the effects of MRGD and MRGDE were studied. In this investigation, the MDA level in the liver tissue homogenate was increased in the LPS-ENR group compared with the BLANK group, suggesting that the liver was occurred oxidative damage. In addition, the capacities of antioxidant enzymes declined significantly with the administration of LPS-

ENR in chicken's liver, and the decreases in SOD and CAT levels confirmed that. When MRGD or MRGDE was administrated, the elevated MDA level was decreased (Figure 5C) and the activities of SOD and CAT were increased (Figure 5D and E).

It is known that the transcription factor Nrf2 plays a central role in antioxidative stress and adjusts lipid metabolism abnormality. Under oxidative stress, Nrf2 dissociated from Keap1 and then transferred into the nucleus, when the Keap1 oxidative modified in the cellular antioxidant defense system (Chen et al., 2019; Chang et al., 2021). Figure 7 showed that the Nrf2/ARE signaling pathway was possibly activated by MRGD and MRGDE. In our study, the results showed that Nrf2 was blocked into the nucleus in the LPS-ENR group (Figure 4), while the transfer of Nrf2, the mRNA expression level of Nrf2, and the protein expression level of Nrf2 were improved by MRGD and MRGDE (Figure 3A and B). Once in the nucleus, Nrf2 bonded to the ARE, thereby activating the mRNA expressions of several downstream genes such as HO-1 and NQO1 in the nucleus (Zhang et al., 2019; Zhao et al., 2020). A report showed that trehalose adjusts the REDOX in cells via activating the Nrf2 pathway and increasing the mRNA expression levels of genes GPX1, CAT, SOD1, NQO1, and HO-1 (Xie et al., 2017). In this research, the mRNA expression levels of HO-1 and NQO1 genes were recovered in the treatment groups, and then activated the mRNA expression of the downstream target genes and the protein expression of GPX1 (Figure 3A and B). The results *in vitro* indicated that MRGD and MRGDE inhibited the accumulation of ROS and increased the accumulation of Nrf2 in the nucleus (Figures 2A and 4). The drugs played an antioxidant activity in the same way as *in vivo* by regulating the Nrf2/ARE pathway

(Figure 6A and B). Therefore, these results suggested that MRGD and MRGDE might be effective in protecting the hepatocytes against oxidative damage.

Liver disease causes more than 2 million deaths annually worldwide (Xing et al., 2021), and about 300 million people suffer from liver diseases in China (Wang et al., 2014); therefore, there has been increasing focus on the burden of severe health. Liver disease has caused a heavy economic burden. RGD is a famous TCM prescription for abdominal pain, which is helpful for the recovery of liver disease and has an unusual application in animals. In this research, the MRGD and MRGDE inhibited the oxidative damage of the liver by activating the Nrf2/ARE pathway. There was almost no difference in the protection effects between the MRGD and MRGDE. The economic cost and cumbersome operation of polysaccharide production were considered, the MRGD was sufficient for liver therapy, and it was unnecessary to further extract polysaccharides.

CONCLUSIONS

In conclusion, when the LPS-ENR caused liver injury, MRGD and MRGDE alleviated the hepatotoxicity and activated the Nrf2/ARE pathway to defend the oxidant stress in vitro and in vivo. The MRGD is more eco-friendly, economical, and simpler than MRGDE to control liver disease.

ACKNOWLEDGMENTS

This work was supported by the National Natural Science Foundation of China (31772784).

DISCLOSURES

The authors declare no conflicts of interest.

REFERENCES

- Albalasmeh, A. A., A. A. Berhe, and T. A. Ghezzehei. 2013. A new method for rapid determination of carbohydrate and total carbon concentrations using UV spectrophotometry. *Carbohydr. Polym.* 97:253–261.
- Al-Dossari, M. H., L. M. Fadda, H. A. Attia, I. H. Hasan, and A. M. Mahmoud. 2020. Curcumin and selenium prevent lipopolysaccharide/diclofenac-induced liver injury by suppressing inflammation and oxidative stress. *Biol. Trace Elem. Res.* 196:173–183.
- Bakr, R. O., M. M. El-Naa, S. S. Zaghoul, and M. M. Omar. 2017. Profile of bioactive compounds in *Nymphaea alba* L. leaves growing in Egypt: hepatoprotective, antioxidant and anti-inflammatory activity. *BMC Complement. Altern. Med.* 17:52.
- Begrache, K., J. Massart, M. A. Robin, A. Borgne-Sanchez, and B. Fromenty. 2011. Drug-induced toxicity on mitochondria and lipid metabolism: mechanistic diversity and deleterious consequences for the liver. *J. Hepatol.* 54:773–794.
- Bi, X. L., M. R. Gong, and L. Q. Di. 2014. Review on prescription compatibility of shaoyao gancao decoction and reflection on pharmacokinetic compatibility mechanism of traditional Chinese medicine prescription based on in vivo drug interaction of main efficacious components. *Evid. Based Complement. Altern. Med.* 2014:208129.
- Chang, B. Y., H. J. Kim, and T. Y. Kim. 2021. Enzyme-treated *Zizania latifolia* extract protects against alcohol-induced liver injury by regulating the NRF2 pathway. *Antioxidants (Basel)* 10:960.
- Chen, L., K. Li, Q. Liu, J. L. Quiles, R. Filosa, M. A. Kamal, F. Wang, G. Y. Kai, X. B. Zou, H. Teng, and J. B. Xiao. 2019. Protective effects of raspberry on the oxidative damage in HepG2 cells through Keap1/Nrf2-dependent signaling pathway. *Food Chem. Toxicol.* 133:110781.
- Cuesta, G., N. Suarez, M. I. Bessio, F. Ferreira, and H. Massaldi. 2003. Quantitative determination of pneumococcal capsular polysaccharide serotype 14 using a modification of phenol-sulfuric acid method. *J. Microbiol. Methods* 52:69–73.
- Gandhi, C. R. 2020. Pro- and anti-fibrogenic functions of gram-negative bacterial lipopolysaccharide in the liver. *Front Med (Lansanne)* 7:130.
- Guo, X. W., W. Y. Li, R. An, M. Huang, and Z. G. Yu. 2020. Composite ammonium glycyrrhizin has hepatoprotective effects in chicken hepatocytes with lipopolysaccharide/enrofloxacin-induced injury. *Exp. Ther. Med.* 20:52.
- He, X. Q., M. G. Chen, and Q. Ma. 2008. Activation of Nrf2 in defense against cadmium-induced oxidative stress. *Chem. Res. Toxicol.* 21:1375–1383.
- He, Y. T., Z. J. Xia, D. Q. Yu, J. K. Wang, L. Jin, D. M. Huang, X. L. Ye, X. G. Li, and B. S. Zhang. 2019. Hepatoprotective effects and structure-activity relationship of five flavonoids against lipopolysaccharide/d-galactosamine induced acute liver failure in mice. *Int. Immunopharmacol.* 68:171–178.
- Hurtado, M., U. T. Sankpal, J. Chhabra, D. T. Brown, R. Maram, R. Patel, R. K. Gurung, J. Simecka, A. A. Holder, and R. Basha. 2019. Copper-tolfenamic acid: evaluation of stability and anti-cancer activity. *Invest. New Drugs* 37:27–34.
- Jadeja, R. N., K. K. Upadhyay, R. V. Devkar, and S. Khurana. 2016. Naturally occurring Nrf2 activators: potential in treatment of liver injury. *Oxid. Med. Cell Longev.* 2016:3453926.
- Jiang, Z. Y., X. M. Zhang, F. X. Zhang, N. Liu, F. Zhao, J. Zhou, and J. J. Chen. 2006. A new triterpene and anti-hepatitis B virus active compounds from *Alisma orientalis*. *Plant. Med.* 72:951–954.
- Krakowian, D., D. Gadarowska, A. Daniel-Wojcik, and I. Mrzyk. 2021. A proposal for a new in vitro method for direct classification of eye irritants by cytotoxicity test – preliminary study. *Toxicol. Lett.* 338:58–66.
- Kucera, O., R. Endlicher, T. Rousar, H. Lotkova, T. Garnol, Z. Drahota, and Z. Cervinkova. 2014. The effect of tert-butyl hydroperoxide-induced oxidative stress on lean and steatotic rat hepatocytes in vitro. *Oxid. Med. Cell Longev.* 2014:752506.
- Lee, H. Y., J. S. Lee, H. G. Kim, W. Y. Kim, S. B. Lee, Y. H. Choi, and C. G. Son. 2017. The ethanol extract of *Aquilariae Lignum ameliore* hippocampal oxidative stress in a repeated restraint stress mouse model. *BMC Complement. Altern. Med.* 17:397.
- Li, J. P., Y. Gao, S. F. Chu, Z. Zhang, C. Y. Xia, Z. Mou, X. Y. Song, W. B. He, X. F. Guo, and N. H. Chen. 2014. Nrf2 pathway activation contributes to anti-fibrosis effects of ginsenoside Rg1 in a rat model of alcohol- and CCl4-induced hepatic fibrosis. *Acta Pharmacol. Sin.* 35:1031–1044.
- Lin, H. R. 2014. Triterpenes from *Alisma orientalis* act as androgen receptor agonists, progesterone receptor antagonists, and glucocorticoid receptor antagonists. *Bioorg. Med. Chem. Lett.* 24:3626–3632.
- Liu, L. S., M. H. Liu, and J. Y. He. 2014. *Hypericum japonicum* Thunb. ex Murray: phytochemistry, pharmacology, quality control and pharmacokinetics of an important herbal medicine. *Molecules* 19:10733–10754.
- Ma, X., W. W. Zhang, Y. X. Jiang, J. X. Wen, S. Z. Wei, and Y. L. Zhao. 2020. Paeoniflorin, a natural product with multiple targets in liver diseases – a mini review. *Front. Pharmacol.* 11:531.
- Peng, X. M., L. Gao, and S. Aibai. 2020. Antifatigue effects of anshenyizhi compound in acute excise-treated mouse via modulation of AMPK/PGC-1 α -related energy metabolism and Nrf2/ARE-mediated oxidative stress. *J. Food Sci.* 85:1897–1906.
- Rabkin, S. W. 2002. Fumonisin blunts nitric oxide-induced and nitroprusside-induced cardiomyocyte death. *Nitric Oxide* 7:229–235.
- Ren, X., L. T. Xin, M. Q. Zhang, Q. Zhao, S. Y. Yue, K. X. Chen, Y. W. Guo, C. L. Shao, and C. Y. Wang. 2019. Hepatoprotective effects of a traditional Chinese medicine formula against carbon tetrachloride-induced hepatotoxicity in vivo and in vitro. *Biomed. Pharmacother.* 117:109190.

- Sun, L., M. Zhao, Y. H. Zhao, M. Wang, J. Y. Man, and C. J. Zhao. 2020. Investigation of the therapeutic effect of Shaoyao Gancao decoction on CCL4-induced liver injury in rats by metabolomic analysis. *Biomed. Chromatogr.* 34:e4940.
- Tang, Y., Y. Xiao, Z. Tang, W. Jin, Y. Wang, H. Chen, H. Yao, Z. Shan, T. Bu, and X. Wang. 2019. Extraction of polysaccharides from *Amaranthus hybridus* L. by hot water and analysis of their antioxidant activity. *Peer J.* 7:e7149.
- Torres, L. R., F. C. Santana, F. L. Torres-Leal, I. L. Melo, L. T. Yoshime, E. M. Matos-Neto, M. C. Seelaender, C. M. Araujo, B. Cogliati, and J. Mancini-Filho. 2016. Pequi (*Caryocar brasiliense* Camb.) almond oil attenuates carbon tetrachloride-induced acute hepatic injury in rats: antioxidant and anti-inflammatory effects. *Food Chem. Toxicol.* 97:205–216.
- Vera-Ramirez, L., P. Perez-Lopez, A. Varela-Lopez, M. Ramirez-Tortosa, M. Battino, and J. L. Quiles. 2013. Curcumin and liver disease. *Biofactors* 39:88–100.
- Vera-Ramirez, L., P. Sanchez-Rovira, M. C. Ramirez-Tortosa, C. L. Ramirez-Tortosa, S. Granados-Principal, J. A. Lorente, and J. L. Quiles. 2011. Free radicals in breast carcinogenesis, breast cancer progression and cancer stem cells. Biological bases to develop oxidative-based therapies. *Crit. Rev. Oncol. Hematol.* 80:347–368.
- Wang, F. S., J. G. Fan, Z. Zhang, B. Gao, and H. Y. Wang. 2014. The global burden of liver disease: the major impact of China. *Hepatology* 60:2099–2108.
- Wu, J. S., Y. F. Li, Y. Y. Li, Y. Dai, W. K. Li, M. Zheng, Z. C. Shi, R. Shi, T. M. Wang, B. L. Ma, P. Liu, and Y. M. Ma. 2017. Huangqi decoction alleviates alpha-naphthylisothiocyanate induced intrahepatic cholestasis by reversing disordered bile acid and glutathione homeostasis in mice. *Front. Pharmacol.* 8:938.
- Wu, P. S., S. J. Wu, Y. H. Tsai, Y. H. Lin, and J. C. Chao. 2011. Hot water extracted *Lycium barbarum* and *Rehmannia glutinosa* inhibit liver inflammation and fibrosis in rats. *Am. J. Chin. Med.* 39:1173–1191.
- Wu, Y. L., S. H. Huang, C. M. He, B. Qiu, J. J. Liu, J. Li, Y. Lin, S. L. Yu, H. F. Wang, and G. F. Zhang. 2020. *Dendrobium officinale* flower extraction mitigates alcohol-induced liver injury in mice: role of antisteatosis, antioxidative, and anti-inflammatory. *Evid. Based Complement. Altern. Med.* 2020:1421853.
- Xi, S. Y., B. Q. Fu, G. J. Loy, G. Y. Minuk, Y. Peng, Y. K. Qiu, X. Y. Zhai, Y. J. Wang, P. F. Li, Y. W. Gong, J. Wang, S. Q. Huang, D. W. Lu, and Y. H. Wang. 2018. The effects of Ciji-Hua'ai-Baosheng on immune function of mice with H₂₂ hepatocellular carcinoma receiving chemotherapy. *Biomed. Pharmacother.* 101:898–909.
- Xie, Y. L., J. G. Chu, X. M. Jian, J. Z. Dong, L. P. Wang, G. X. Li, and N. B. Yang. 2017. Curcumin attenuates lipopolysaccharide/d-galactosamine-induced acute liver injury by activating Nrf2 nuclear translocation and inhibiting NF-kB activation. *Biomed. Pharmacother.* 91:70–77.
- Xing, Y. Y., Y. K. Zheng, S. Yang, L. H. Zhang, S. W. Guo, L. L. Shi, Y. Q. Xu, X. Jin, S. M. Yan, and B. L. Shi. 2021. *Artemisia ordosica* polysaccharide alleviated lipopolysaccharide-induced oxidative stress of broilers via Nrf2/Keap1 and TLR4/NF-kappaB pathway. *Ecotoxicol. Environ. Saf.* 223:112566.
- Yi, P., N. Li, J. B. Wan, D. Zhang, M. Li, and C. Yan. 2015. Structural characterization and antioxidant activity of a heteropolysaccharide from *Ganoderma capense*. *Carbohydr. Polym.* 121:183–189.
- Yuan, R. S., X. Tao, S. Liang, Y. Pan, L. He, J. H. Sun, W. B. Ju, X. Y. Li, J. G. Chen, and C. M. Wang. 2018. Protective effect of acidic polysaccharide from *Schisandra chinensis* on acute ethanol-induced liver injury through reducing CYP2E1-dependent oxidative stress. *Biomed. Pharmacother.* 99:537–542.
- Zhang, S. L., X. L. Yi, X. Su, Z. Jian, T. T. Cui, S. Guo, T. W. Gao, C. Y. Li, S. L. Li, and Q. Xiao. 2019. Ginkgo biloba extract protects human melanocytes from H₂O₂-induced oxidative stress by activating Nrf2. *J. Cell. Mol. Med.* 23:5193–5199.
- Zhang, X., Y. Xu, J. M. Chen, C. Liu, G. L. Du, H. Zhang, G. F. Chen, S. L. Jiang, C. H. Liu, Y. P. Mu, and P. Liu. 2017. Huang Qi decoction prevents BDL-induced liver fibrosis through inhibition of notch signaling activation. *Am. J. Chin. Med.* 45:85–104.
- Zhao, B. C., Z. J. Wang, J. G. Han, G. H. Wei, B. Q. Yi, and Z. L. Li. 2020. Rhizoma *Paridis* total saponins alleviate H₂O₂ induced oxidative stress injury by upregulating the Nrf2 pathway. *Mol. Med. Rep.* 21:220–228.
- Zhao, S. P., Z. S. Wu, Y. Chen, X. Liang, L. Bao, P. Li, R. R. Sun, Y. L. Wu, L. R. Li, and Q. Wang. 2017. Protective effect of Hua Tan Qu Shi decoction against liver injury in rats with nonalcoholic fatty liver disease. *Biomed. Pharmacother.* 91:181–190.